APTAMERS AS A METHOD FOR THYROID CANCER DIAGNOSIS

Victor Souob

Research report submitted to the department of Biochemistry, Microbiology and Immunology in partial fulfillment of the requirements for the course BCH 4040

University of Ottawa

Ottawa, Ontario, Canada

April 2014

Abstract

Diagnosis of differentiated thyroid cancer (DTC) has been a major problem in the past few decades. In fact, immunometric assay (IMA) and radio-immunometric assay (RIA) are current methods of diagnosis using exogenous antibodies against serum thyroglobulin (Tg), a cancer marker. About 30% of DTC patients produce endogenous Tg auto-antibodies (TgAb) that bind to serum Tg at the same binding site as RIA and IMA exogenous antibodies. As a consequence, when RIA and IMA are used for diagnosis, the Tg levels are often underestimated. To overcome this obstacle, we offer a novel method of diagnosis by testing a pool of aptamers (single-stranded DNA sequences which act like antibodies) previously selected against Tg in the presence of TgAb. The pool was selected using the SELEX procedure followed by sequencing and affinity analysis. From this, 3 specific aptamers (apt1, apt2 and apt3: figure 2) were isolated from the DNA pool as possible candidates for targeting Tg. Finally, binding analysis of the three aptamers was measured using flow cytometry. As a result, all 3 aptamers were found to bind more specifically to Tg than the negative control (nonspecific ssDNA). However apt3 (saturated Tg at 200nM) show a higher affinity to Tg than apt1 and apt2 (both saturated Tg at 500nM). Suggesting that apt3 has the lowest KD of all the 3 aptamers and seems to be the best candidates for DTC diagnosis. Future work will involve confirmation of this result using statistical analysis as well as diagnosis with human serum in the presence of TgAb. Thus, apt3 isolated from a pool selected in the presence of TgAb seems to bind Tg successfully in vitro suggesting that apt3 is a possible candidate for DTC diagnosis. This can lead to a novel approach of biosensing differentiated types of thyroid cancer.

Acknowledgment

All my gratitude goes to Dr. Maxim V. Berezovski for giving me the opportunity to be part of his research group during the eight months of my honours project.

I would like to thank Dr. Pavel Milman for his continuous support and for the time that he spent to train me. I would also like to thank the rest of the Berezovski research group especially Nadia Al-Youssef, Darija Muharemagic and Ana Gargaun for their continuous help.

I would finally like to thank my family for their help and support especially my parents Samuel and Chantal Souob, my friends Alaa Ali, Koby Ampofo and Dr. John Basso.

Table of Contents

List of figures

Contribution Statement

Conception:

My supervisor Dr. Maxim V. Berezovski had the idea and the conception of aptamers selections for thyroglobulin.

Writing:

This thesis was written by Victor Souob.

Experimental:

The SELEX protocol (figure: 1) was performed by Ali Farhan (a previous honours student). The aptamers pool (figure: 2) was sequenced by ACGT Sequencing in Montreal. Amplification and purification of the pool as well as the binding test analysis of the aptamers to the thyroglobulin was performed by Victor Souob (figures 4-13).

Introduction:

I- Thyroid Cancer

A-Origin and prevalence of Thyroid cancer

Thyroid cancer was considered a rare cancer just a decade ago. Since then, the rate of incidence has inclined for an unknown reason. According to the World Health Organization and the Canadian Society of Cancer, the incidence of thyroid cancer worldwide is now estimated at 213,000 individuals per year (WHO, 2012) and it is the most prevalent cancer among Canadian young women (PHAC, 2011). In 2011 alone, an estimated 5, 600 patients were newly diagnosed with thyroid cancer in Canada (PHAC, 2011).

Thyroid cancer is the most frequent endocrine cancer and can be defined as a malignant neoplasm originating from the follicular (95-97%) or parafollicular (3-5%) thyroid cells (Nikiforov et al, 2009). The follicular cell-derived cancers are subdivided into diver's type. The well-differentiated papillary carcinoma and follicular carcinoma, the poorly differentiated carcinoma, and the anaplastic carcinoma (DeLellis et al, 2004).

Follicular cells are thyroid epithelial cells responsible for the production and secretion of thyroglobulin hormones (Walter F, 2003). In parallel, parafollicular cells are neuroendocrine cells present in the thyroid which secrete calcitonin (Zabel M, 1984). A dysfunctional follicular or parafollicular cells can directly lead to thyroid cancer. Over 90% of thyroid cancers are originating from the follicular or papillary cells, better known as differentiated thyroid cancer (DTC) (Davies L, 2006).

Specific point mutations of certain genes can lead directly to thyroid cancer. For example most mutations in thyroid cancer involve the effectors of the mitogen-activated protein kinase (MAPK) and the Phosphoinositide 3 kinase-Protein kinase B (PI3K-AKT) pathways (S. Libero et al, 2008). In fact, MAPKs are important signal-transducing enzymes involved in the regulation of cell proliferation, cell death and genes expression (L. Chang and M. Karin, 2001). Continuous activation of MAPKs due to point mutation of specific genes (BRAF, RAS and RET genes) can lead directly to thyroid cancer (Yamashita et al, 2013). In fact, common mutations found in thyroid cancer are the Val600Glu amino acid substitution in the protein BRAF (Xing, 2005) and a mutation in the protein RAS (Suarez et al, 1990). BRAF is a serine protein kinase while RAS is a G protein present in the inner site of the cell membrane.

In parallel, the PI3K-AKT cell signaling pathway is responsible for cell proliferation, cell migration and cell resistance to apoptosis (Cully et al, 2006). Mutations in the gene encoding the Class I PI3K catalytic subunit (PIK3CA) is also described in thyroids cancer (Hou et al., 2007). In addition, exposures to specific chemical compounds found in volcanic areas can also lead to thyroid cancer via mutagenesis (Parkin et al, 2005).

There is currently no known preventive action that can be taken to avoid being afflicted with DTC. In fact, the survival rate of DTC is 90% during 10 years but recurrences can occur in 25% of the cases, sometimes 30 years after the first diagnosis and it is imperative to regularly check patients with DTC during their lifetime (Tubiana et al, 1985). However, some therapies are available for thyroid cancer treatment. In fact, radiation therapies and surgical removal of the thyroid gland can be applied to cure thyroids cancer but patients without thyroid gland should remain on thyroglobulin treatment for the rest of their lives (Schlumberger et al, 2004). In

addition, thyroglobulin serum measurement plays a crucial function for the diagnosis of thyroids cancer (Spencer, 1998).

B-Synthesis and function of Thyroid Hormones

Thyroglobulin (Tg) is a dimeric glycoprotein of 670 kilodalton (kDa) synthesized by thyroid follicular cells which undergoes multiple posttranslational events including glycosylation, iodination and phosphorylation (Spencer et al, 1998). Tg is specific to thyroid tissue (Tg is not biologically active) and is the substrate of the thyroid hormones thyroxine (T4) and triiodothryronine (T3) which are involved in the metabolism in almost every tissue in the body (Yves Malthiéry et al, 1989). In fact, T4 and T3 are essential hormones and synthetic T3 and T4 hormones must be given to patients who had their thyroid gland removed (Deshpande, 1999). In addition, thyroglobulin and thyroid are important storage of iodine for all body needs, especially for iodine-concentrated organs such as breast, salivary glands, and thymus (S.Venturi et al, 2000).

Tg synthesis (figure 1 appendix) are made by follicular thyroid cells and their functions include the uptake of iodine and amino acids from the blood, the synthesis of Tg and secretion of thyroxine (T_4) and triiodothyronine (T_3) into the blood (Boron WF, 2003). However, in athyroid individuals Tg concentrations are very low or undetectable, but elevated or rising serum Tg levels are suspicious of recurrent or persistent disease in DTC (Cooper DS et al, 2009). Thus, Tg serum measurements can be used as a tumor marker (Cooper DS et al, 2009).

C-Diagnosis of thyroid cancer (DTC)

Overall, the main problem of DTC type of cancer remains the diagnosis. To diagnose DTC, exogenous antibodies are delivered against the serum of DTC patients to measure the serum level of Tg, the cancer marker. In fact, values lower than 22 IU/mL (Tg serum level) are considered normal (JI Torrens et al; 2001). The diagnosis can be performed using an immunometric assay (IMA) or radio-immunoassay (RIA) (JI Torrens et al; 2001). However, 30% of DTC patients produce endogenous Tg auto-antibodies (TgAb) that bind to Tg in the serum (Spencer, 2004). In this case, IMA and IRA assays are unreliable due to the presence of the TgAb that competes with the exogenous antibodies for the same epitopes (Spencer 2004) (figure 3). Thus, in the presence of TgAb, the serum measurement of Tg is underestimated and this interference has been identified as the "most serious technical problem that currently compromises the use of serum Tg as a tumor marker test for patients with DTC'' (Spencer, 2008). Different clinical methodologies have been used so far to measure Tg level in presence of TgAb in the serum but the diagnostic tests were shown to differ from one another leading to erroneous clinical interpretation (JI Torrens et al; 2001).

II-Aptamers

A-Definition

Aptamers can be defined as synthetic antibodies (Jayasena 1999). They are generally oligonucleotides, single-stranded nucleic acids (ssRNA or ssDNA) capable to bind specific target

molecules with high affinity and specificity (Jayasena 1999). In vivo, aptamers naturally exist in riboswitches which are found to be regulatory segment of messenger RNA that specifically bind small molecules resulting in a change in the expression of the protein encoded by the messenger RNA (Vitreschak AG et al, 2004). In addition, aptamers fold in specific structural conformation in order to bind their target with high specificity and affinity (Jayasena, 1999). In fact, aptamers can generate many conformational structures such as stems, loops, bulges, which arise from intramolecular interactions like hydrogen bound between complementary bases (Z.Huang, 2003).

In vitro, aptamers are generated by a protocol called SELEX (systematic evolution of ligands by exponential enrichment) (Gold, 2000). As shown in figure 1, SELEX protocol consists initially of a negative selection where non-specific aptamers are discarded from the initial DNA library (Gold, 2000). This is followed by a positive selection, in which the target is incubated with aptamers that will potentially bind to the target (Gold, 2000). The last step consists of PCR amplification of the selected aptamers that bind specifically to the target followed by subsequent round of SELEX (up to 10 rounds) (Gold, 2000). Upon completion, affinity analysis and sequencing are made from the pool that shows a higher affinity for the target (Gold, 2000). Also, computer analysis of the pool identifies the specific sequences of the aptamers (D.A Daniels et al, 2003) (figure 2). In addition, the ssDNA library used by the SELEX protocol can be generated by combinatorial chemistry which can generate up to 10^{13}-10^{15} large pools of DNA with different specific sequences and structures (Osborne, S. E et al; 1997). In fact, this can be explained by assuming that each ssDNA present in the pools contains a central randomised region of 40-60 nucleotides flanked by regions containing the primers sequences (approximately 20 nucleotides) necessary for the polymerase chain reaction (PCR).

Since nucleic acids are composed of 4 different nucleotides, we can conclude that theoretically between 4^{40} to 4^{60} individual sequences can be generated using the SELEX protocol. With this large amount of individual sequences, we can assume that at least one of them will bind to their selected target during the SELEX procedure. In fact in the past decade, different aptamers have already been selected for a variety of targets including dopamine (Walsh, R et al; 2009), interferon-gamma (Min, K et al; 2008) and lysozyme (Potty, A et al; 2009).

In addition, aptamers can also be used for therapy purposes (Proske, D et al; 2005). Compare to antibodies, aptamers have many qualities that make them good tools for biosensing and therapy. For therapy, aptamers can be easily modified with a D-nucleotide during their synthesis in order to increase their stability against nucleases (which recognize L-nucleotides) and their affinity when used in vivo (Sundaram, 2013). Also, aptamers can be selected for many ranges of target and can also be easily conjugated with a fluorophore during biosensing when comparing to antibodies (Yun, M et al; 2011). In fact, it`s difficult even sometimes impossible to conjugate some antibodies with a fluorophore and conjugation can lead in some case to a defective antibody or to a reduction of affinity (Jayanesa 1999).

B-Aptamers for recognition of biomarkers

Aptamers can be selected directly to bind biomarkers (proteins specific for cancer) present in the serum (Walsh, R et al; 2009). One specific example is the biomarker for prostate cancer. Here, the prostate epithelium produces the biomarker Prostate Specific Antigen (PSA), a glycoprotein which is released into the bloodstream of cancer patients (Yun, M et al; 2013). In fact, one aptamer has been successfully selected for PSA. This specific aptamer is now used as a biosensor for prostate cancer (Yun et al, 2013).

As mentioned, in DTC 30% of the cases TgAb auto-antibodies are found and this seems to underestimate the serum measurement of Tg especially when IMA or RIA are used since both methods of measurement depend on exogenous antibody. However, guided by the quality of aptamers, we are stating that selecting an aptamer that is capable of binding Tg on a different epitope or with a higher affinity than the TgAb auto-antibodies will overcome this obstacle (figure 3). Therefore, a successful result here will generate aptamers that bind Tg in a different binding site or with better affinity than Tg-Ab. Such result will certainly overcome the obstacle found in the presence of TgAb and will lead to a novel approach of biosensing DTC. In fact, the aim of this study is to test the binding affinity of 3 specific aptamers for Tg and measure their respective dissociation constant (K_d). The 3 aptamers were obtained from a pool of aptamers previously selected against Tg in the presence of TgAb. The pool was selected using the SELEX protocol. Sequencing and affinity analysis were performed to generate the 3 aptamers (apt1, apt2 and apt3: figure 1).

Materials and Methods

DNA Library

The DNA libraries used in this project were purchased from Havard DNA library (integrated DNA technologies Inc). They are single stranded DNA of 100 oligonucleotides in length, consisting of two flanking primer regions of 20 nucleotides each. The left 60 random nucleotides is the center region which creates the diversity.

PCR amplification

A symmetric PCR was performed and double stranded DNA (dsDNA) was obtained as final product. Initially 5 ul of a pool of aptamer selected against Tg coupled to monoclonal Tg antibody (mAb Tg) was mixed with 45 ul of symmetric PCR master mix. The master mix contained the following reagents at their final concentration : 5x Kappa 2G GC buffer with 1.5 mM Mg^{2+} at 1x (promega corporation), 5u/ul of GoTaq Hot start polymerase (promega corporation), 10 mM dNTPS , 10uM forward Cy5-primer (5'-Cy5-CTCCTCTGACTGTAACCACG-3') (integrated DNA technology) , and 10 uM reverse primer (5'-GGCTTCTGGACTACCTATGC-3'). Amplification was performed using the following program: preheating for 2 min at 95 ^{o}C, 15 cycles of PCR for 30 sec at 95 ^{o}C, 15 sec at 56.3 ^{o}C, 15 sec at 72 ^{o}C, and was held at 4 ^{o}C after completion.

To obtain single stranded DNA (ssDNA), asymmetric PCR was performed. Upon completion, 5 ul of the symmetric product was added to 45 ul of the asymmetric PCR master mix which contains the same reagents as the symmetric master mix but with a higher concentration (10 uM) of the forward Cy5 -primer (5'-Cy5-CTCCTCTGACTGTAACCACG-3') and 500 nM of the reverse primers (5'-GGCTTCTGGACTACCTATGC-3'). Here, we used a higher concentration

of forward primers to generate only the ssDNA (aptamer). Amplification was performed using the following program: preheating for 2 min at 95 ^{o}C, 10 cycles at 58^{o}C for 30 sec (15 sec. heating at 94 ^{o} C for denaturation, 10 sec. annealing at 58^{o} C and 5 sec. elongation at 72 ^{o} C), 10 cycles at 57 ^{o} C for 30 sec ,and 20 cycles at 56 ^{0} C for sec. The final PCR product was held at 37 ^{o} C after completion.

DNA purification

Asymmetric product from the PCR was excised off the gel (3 %) and was incubated in water overnight at 4^{0}C to permit the DNA to diffuse. After incubation, DNA concentration was obtained following the Amicon® Ultra-05 centrifugal filter devices protocol.

Concentration of the purify DNA

After purification, concentration of the purified DNA was estimated using a gel ladder with different concentration of DNA. Thus, the intensity of the purified DNA was compare to the ladder to estimate the concentration.

Aptamer Sequencing

The aptamer pool was sequenced by AGCT (Montreal) as follow: The aptamer pools were treated to blunt and the ends was phosphorylated and ligated into concatamers. NexteraXT sample prep kit was used to generate randomized indexed libraries (thus avoiding the need for adapters and PCR). The libraries were run on MiSeq, generating about 0.5 million paired end reads per pool on average (after filtering short reads or reads with insertions into the randomized region). Individual 40 bp randomized sequences were then binned, and a report was generated with pool compositions (aptamer sequence vs. difference of reads).

Coupling of protein to magnetic beads

70 ul (5mg/ml) of thyroglobulin were washed 2 times (following the Amicon® Ultra-05 centrifugal filter devices protocol) with 100 ul of activation/coupling buffer 2-(N-morpholino)-ethanesulfonic acid (MES) (sigma) (A/C buffer) and was stored at 4^{o} C. Also, 100 ul of pureProteome ^{TM} Carboxy Flexibind Magnetics Beads (Millipore) were washed 3 times with 200 ul of A/C buffer and were incubated with 20 ul of 1-ethyl-3-(3 dimethylaminopropyl) carbodiimide hydrochloride (EDC) (50 mg/ml) (sigma) in 80 ul of A/C buffer for 30 minutes with slow rotation at room temperature. Following the incubation, beads were washed with 100 ul of A/C buffer and were immediately incubated with 350 ug of thyroglobulin (sigma) pre-washed in 100ul of DPBS $Mg^{2+}Ca^{2+}$ 0.005 % Triton for 3 hrs. After incubation, the supernatant was discard and beads newly coupled to protein were incubated with 500 ul of TBS (25mM Tris-Cl, 130 mM Nacl, 2.7 mM KCl), pH 8, 0,01% Triton ® X-100 (quench buffer) for 30 minutes with slow rotation at the room temperature. Additionally five washes were made after incubation with quench buffer and beads coupled to thyroglobulin were stored in 100 ul of DPBS $Mg^{2+}Ca^{2+}$ 0.005 % Triton at 4 ^{0}C.

Coupling Tg monoclonal antibodies (Tg mAb) to Tg-beads

10 ul of beads coupled with Tg were initially washed twice with D-PBS Mg^{2+} Ca $^{2+}$ 0.005 % Triton and were incubated for 30 minutes with slow rotation at room temperature with 1 % bovine serum albumin (BSA) (in 300 ul of D-PBS Mg^{2+} Ca $^{2+}$ 0.005 % Triton) for blocking. Upon completion, 1.5 ul (0.2 mg/ml) of Tg monoclonal antibodies were directly added to the solution and the mix was incubated for an additional 30 minutes. After incubation the beads-Tg newly coupled with the monoclonal Tg antibody were washed 5 times with DPBS Mg^{2+} Ca $^{2+}$

0.005 % Triton with shaking for 3 min and were suspended in 400 ul for flow cytometry. The same protocol was used for the negative controls which are beads coupled with human myeloperoxidase protein (MPO) and beads alone.

Affinity analysis of aptamers to thyroglobulin

Tg-beads and beads alone were incubated with different concentrations of apt1, 2 and 3 in 200 nM, 500nM and 1 uM DPBS Mg^{2+} Ca^{2+} 0.005 % triton respectively with slow rotation at the room temperature for 1 hr. Upon completion, they were washed 5 times with DPBS Mg^{2+} Ca^{2+} 0.005 % Triton and were suspend in 400 ul of DPBS Mg^{2+} Ca^{2+} 0.005 % for flow cytometry. The same protocol was used for the negative control which is forward CY5- primer (5'-Cy5-CTCCTCTGACTGTAACCACG-3')

Flow Cytometry :

Affinity analysis of aptamers and coupling Tg mAb to Tg-beads was measured using FC-500 flow cytometer (Bechman Coulter Inc) .

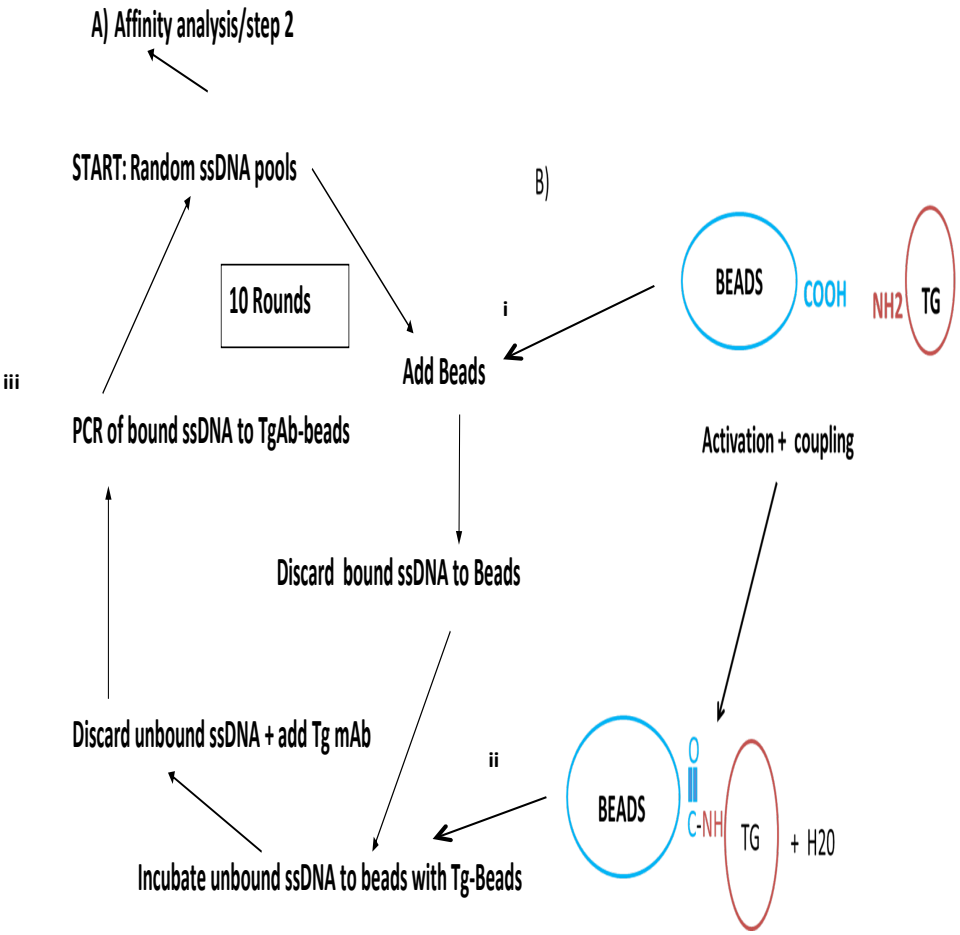

Figure:1. A) Selection of DNA aptamers to TgAb . The SELEX procedure consist of 10 rounds iterating 3 major steps: (i) negative selection of ssDNA to beads, (ii) positive selection of ssDNA to Tg-beads, and (iii) PCR amplification. Selected aptamer pools are analyzed by flow cytometry and the best pool is cloned and sequenced. **B) Representation of the coupling of carboxyl beads to Tg.** The carboxyl group on the beads surface reacts with the N-terminal region of Tg which leads to the formation of beads covalently bound to Tg.

Aptamer 1:

5’−TTGCAGTACAGCGACAATACCGCCATGACAAATTGATTGCCCAGCTCGGTGGCCCGGGAGGCGTGACAC−3’

Aptamer 2:

5’−CGTTTGAATCTCCCCGGCCGCAATTTGACCGCACCGCCGGCAAACGGCCCGTACG−3’

Aptamer 3:

5’−CTGGGAATTCTTTGCACGTTATCGCACTGCCACGACCAGAGTTTGCCCGGACGGACAAACGGCCGACCAC−3’

Figure2. DNA sequences of aptamer 1 (apt1), 2 (apt2) and 3 (apt3) that were isolated from a binding pool to Tg coupled with TgAb following the 3rd round of SELEX. Sequencing of the pool was performed by ACGT sequencing in Montreal. Computer analysis was used to test the binding affinity of each aptamer to Tg. Thus, apt1, 2 and 3 were isolated as the best candidates.

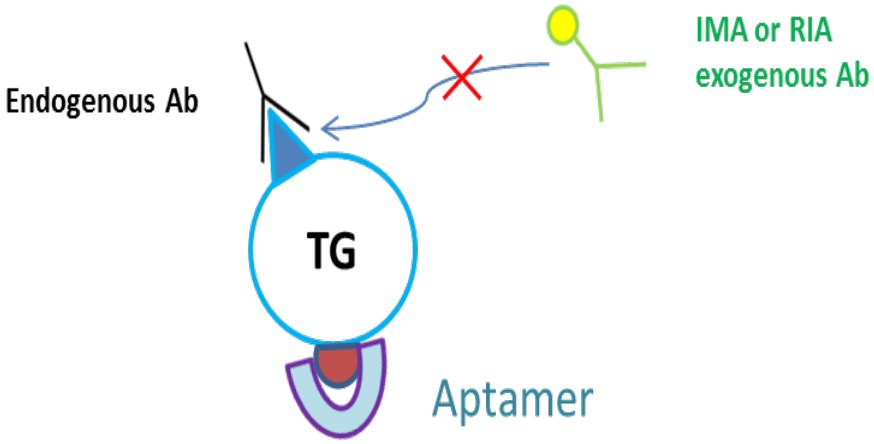

Figure:3. Hypothetical graphic representation of aptamer bound to Tg in the presence of endogenous antibody (TgAb). Because endogenous antibodies bind the Tg at the same epitope as IMA (or RIA) exogenous antibody (in green), the latter cannot bind to Tg. This leads to an underestimation of Tg levels during diagnosis in 30 % of the cases. However, selecting an aptamer (in blue) that is able to bind a different region of Tg could avoid this underestimation.

Results

Coupling magnetics beads to Thyroglobulin (Tg)

Coupling of magnetics beads to Tg was successful. As show in figure 4, the highest mean of fluorescent intensity (MFI: 10.23) is observed when FITC labeled monoclonal thyroglobulin antibody (mAb Tg) is incubated with beads coupled to Tg (beads-Tg) as compared to the negative controls: beads coupled with MPO (MFI: 4.24) and beads alone (MFI: 4.77). To determine whether this difference was significant, the experiment was performed in triplicates in order to determine p values (experiment with MPO was only performed once). A p value of 0.0003 was obtained when Tg-beads was compared to beads in the presence of mAb Tg. In addition, a significant shift (p value 0.0041) of MFI was observed when beads-Tg in the presence of mAb Tg were compared to beads-Tg in the absence mAb Tg (MFI: 6.03). Also a p value of 0.0005 was obtained when the latter was compared to beads alone (MFI: 0.17).

Comparative affinity analysis of aptamers 1, 2 and 3(apt1, 2and 3) to beads-Tg and beads.

All 3 aptamers were incubated at different concentration (200nM, 500nM and 1 uM) with beads coupled to Tg and beads alone to test if they were selected against Tg or the beads. For all 3 aptamers, apt3 seems to be the best aptamer selected against Tg. In figure 5A, we observe that apt1 incubated with beads-Tg has the highest MFI at 500 nM (3.2). At 1 uM the MFI of apt1 decrease to 2.62 and it is slightly higher to the uncoupled beads (2.57). However the MFI of apt1 to uncoupled beads increase slightly as we increase its concentration (2.18, 2.35 and 2.57 at 200nM, 500nM at 1uM respectively).

In figure 5B, at 200nM the MFI of apt1 incubated to beads-Tg and to uncoupled beads is slightly different (2.41 and 2.18 respectively) but as we increase the concentration of ap1 we observe an increase of the trend line for beads-Tg (slope: 0.0026) as compared to the uncoupled beads (slope: 0005) when affinity analysis were compared at 200 and 500nM only.

With apt2 (figure 6A) we also observe a highest MFI at 500 nM (3.075) for beads-Tg (2.72 as compared to MFI of uncoupled beads at 500 M). However at 1uM the MFI of apt2 decreases to 2.78 and is somewhat similar to the uncoupled beads (2.85). Also the trend of the MFI for the uncoupled beads seems to be similar as we increase the concentration of apt2 (2.77, 2.72 and 2.78 at 200nM. 500nM and 1uM respectively) while for beads-Tg it's slightly differ (especially at 500nm). In figure 6B we observe a higher increase of the trend line for beads-Tg (slope : 0.0007) as compared to the uncoupled beads (slope ; -0.0002) when affinity analysis were compared at 200 and 500nM only.

When incubated with beads-Tg, apt3 shows the highest MFI at 200nM (2.9) (figure 7A). But at 500nM the MFI dropped to 2.67 and changed slightly at 1uM (2.74). The trend of the MFI for the uncoupled beads, when incubated with apt3, changed considerably as we increase its concentration (1.9, 2.62, and 3.23 at 200nM, 500nM and 1uM respectively). In figure 7 B we observed a higher increase of the trend line for uncoupled beads (slope: 0.0021) as compared to beads-Tg (slope: - 0.0007) when affinity analysis were compared at 200 and 500nM only.

To determine whether this difference was significant, all experiments were performed in triplicates in order to be able to measure p values. Statistically significant shift of MFI with all 3 aptamers after triplicate of each experiment was not obtained. Nevertheless a statistical significance was almost reached with apt3 at 200nM (p=0.0843, figure 7A).

Affinity analysis of apt 1,2 and 3 to beads-Tg and to a nonspecific* ssDNA *control

All 3 aptamers plus a nonspecific ssDNA (control) were incubated at different concentration (200nM, 500nM and 1 uM) with beads coupled to Tg to see their specificity to Tg. For all 3 aptamers, apt3 seems to be the most specific to Tg. In figure 8, at 200nM all 3 aptamers seem to bind more the beads coupled to Tg than the nonspecific ssDNA control (MFI of 2.02). However at 500nM (figure 9), only apt1 and apt 2 (MFI: 3.20 and 3.075 respectively) seem to bind more Tg than the control and apt3 (both showing quite similar binding). Finally at 1uM (figure 10) all 3 aptamers and the control seem to bind Tg in a similar way. a statistically significant shift of MFI with all 3 aptamers after triplicate of each experiment was not observed. In fact the lowest p value (0.182) was observed with apt3 (figure 8) at 200nM.

In order to measure the K_d, the trend of the binding affinity of all 3 aptamers and the control (all incubated with Tg-beads) was analyzed at different concentration (200nM, 500 nM and 1 uM). For all 3 aptamers, apt3 seems to have the highest affinity to Tg . In figure 11, we observe that apt3 (in red) shows a higher MFI to Tg only at 200nM as compared to the control (F4 in blue). But at 500nM the MFI of apt3 decrease (MFI is found to be under the trend line). Finally at 1 uM the MFI of apt3 is quite similar to the control. In figure 12 and 13, we observe that apt2 and apt1 have a higher MFI to Tg at 200nM and 500nM (at 500nM both MFI are found to be on top of the trendline) but at 1 uM the MFI of both decrease (under the trend line) and seems to have a similar or lower MFI when compared to the control F4. Finally, the trend line illustration the MFI of the non-specific ssDNA (figure 10, 11 and 13) increased gradually as we increased its concentration ($R^2 = 0.9315$)

Results

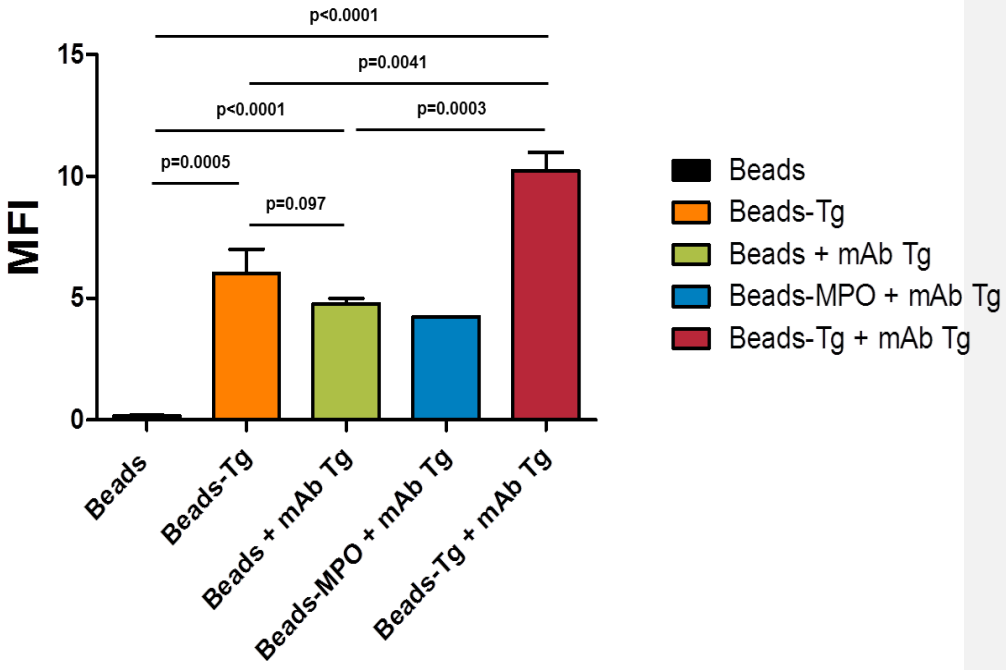

Figure 4 : **Flow cytometric analysis of FITC-labeled Tg antibody against Tg (mAb Tg) coupled with magnetic beads**. 1.5 ul (0.2mg/ ml) of FITC-labeled anti-rabbit IgG antibody to thyroglobulin was incubated with 10 ul of Tg-coupled with magnetic beads, beads alone and beads coated to MPO with 1 % BSA in 300 ul of DBPS $Mg^{2+}Ca^{2+}$ 0.005% Triton. In the presence of mAb Tg, beads coupled with Tg (red) show a significantly higher mean fluorescence intensity (MFI of 10) compared to negative controls, MPO-beads (blue) and beads alone (green) (MFI of 4.24 and 4.77 respectively) . ***Experience with MPO beads was only performed once

A)

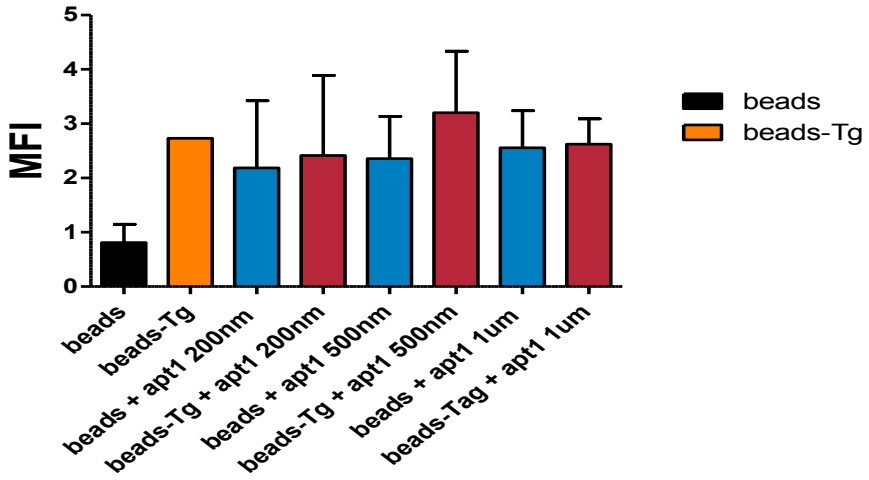

B)

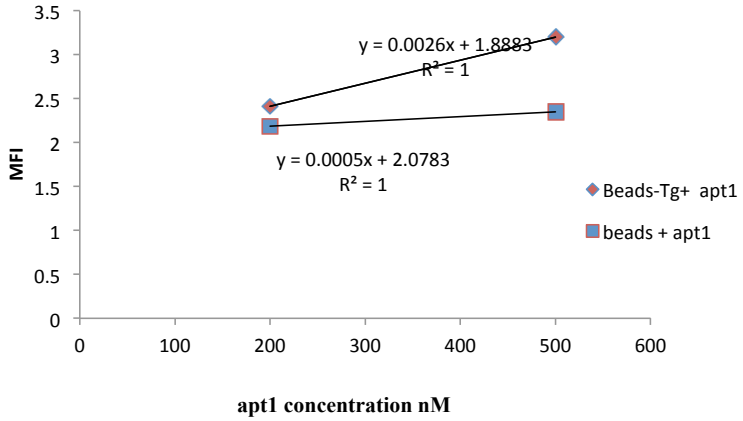

Figure:5: ***A)*** **Flow cytometric analysis of aptamer 1 (apt1) affinity to Tg**. Comparative binding of apt1 at different concentration (200nM , 500nM and 1uM) to beads coupled with Tg (red) and beads alone (blue). Apt1 were labeled with the Cy5 dye at the 5' end. Here, apt1 show his highest MFI at 500nM. ***B)*** **Scatter plot illustrating the comparative binding of apt1 to Tg-Beads and beads only at 200nM and 500nM**. Here, apt1 show a higher affinity to bead-Tg than to beads alone

A)

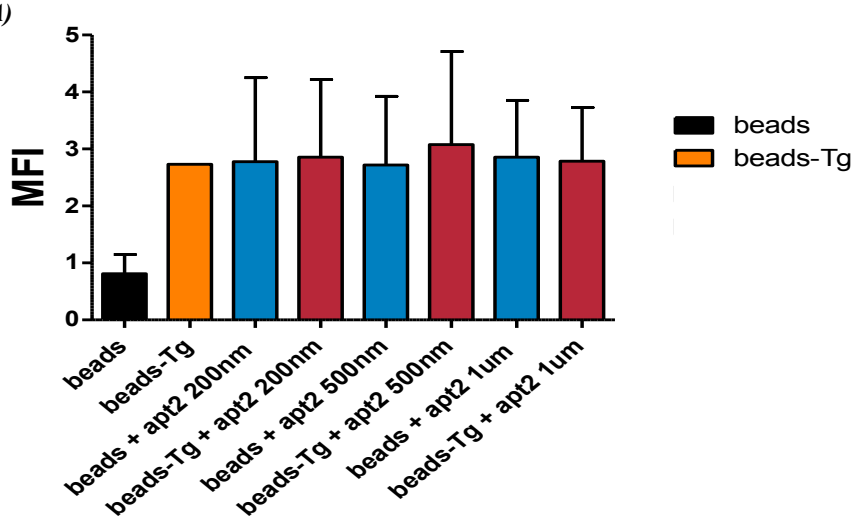

B)

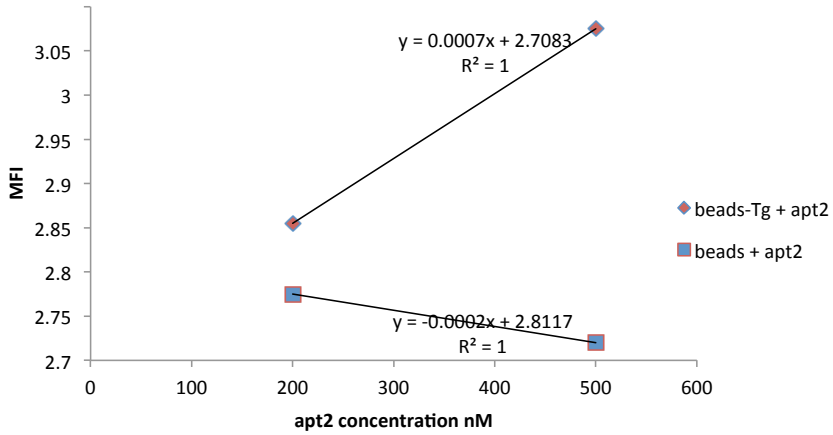

Figure: 6: ***A)*** **Flow cytometric analysis of aptamer 2 (apt2) affinity to Tg**. Comparative binding of apt2 at different concentration (200nM , 500nM and 1uM) to beads coupled with Tg (red) and beads alone (blue). Apt2 were labeled with the Cy5 dye at the 5' end and comparative binding was tested by flow cytometry.As result, apt2 seems to have his highest MFI at 500nM. ***B)*** **Scatter plot illustrating the comparative binding of apt2 to Tg-Beads and beads only at 200nM and 500nM**. Here, apt2 seems to show a higher affinity to beads-Tg than to beads alone

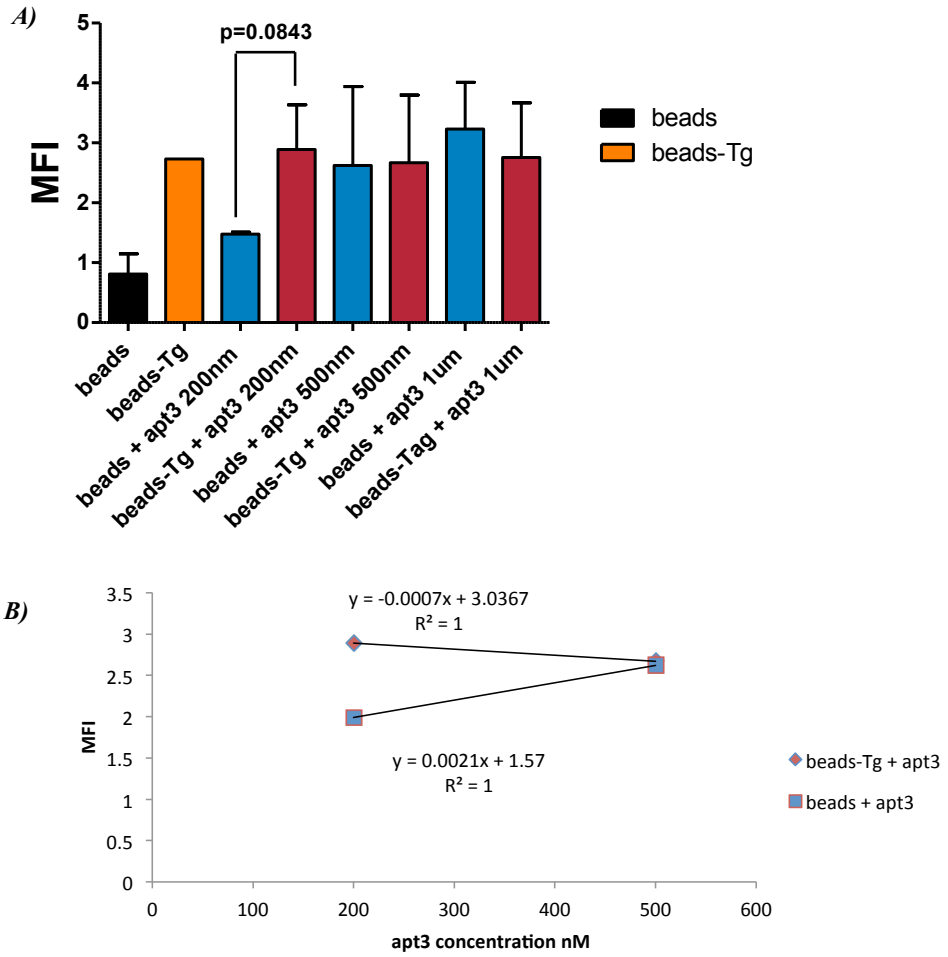

Figure: 7: ***A)*** **Flow cytometric analysis of aptamer 3 (apt3) affinity to Tg**. Comparative binding of apt3 at different concentration (200nM , 500nM and 1uM) to beads coupled with Tg (red) and beads alone (blue). apt3 were labeled with the Cy5 dye at the 5'.As result apt3 show his highest MFI at 200nM***B)*** **Scatter plot illustrating the comparative binding of apt3 to Tg-Beads and beads only at different concentration** (200nM and 500nM). At 200nM apt3 (red) show a higher affinity to beads-Tg than beads alone (blue), but show similar affinity to beads-Tg and uncoupled beads at 500nM.

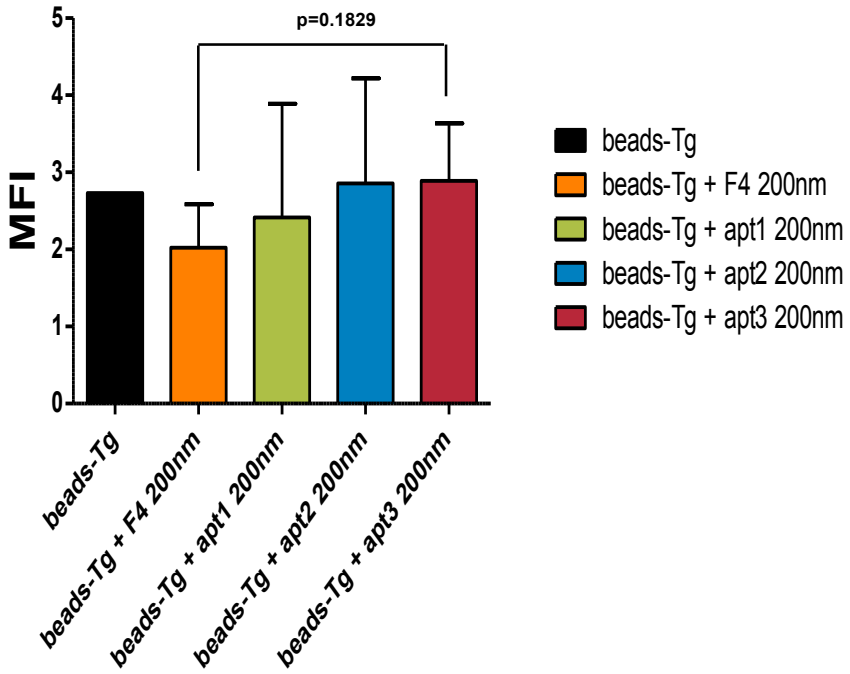

Figure 8: Flow cytometric analysis of apt1, 2 and 3 (ssDNA) affinities to Tg. Affinity analysis of apt1, 2 and 3 to beads coupled with Tg (green, blue and red respectively). A concentration of 200 nM of aptamers was used. Aptamers were labelled with the Cy5 dye at the 5' end. A nonspecific ssDNA (F4; yellow) was used as a control (also laballed with Cy5) . All 3 aptamers show a higher MFI to beads-Tg than the control F4 at 200nM.

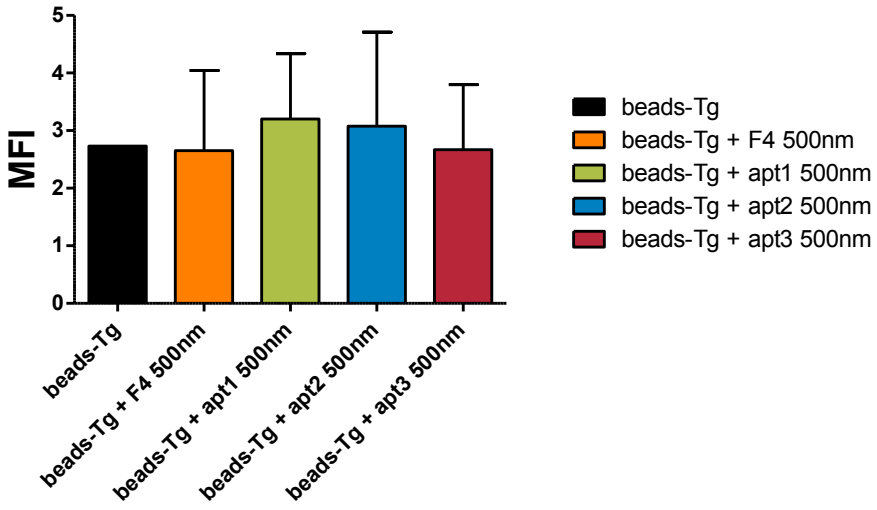

Figure: 9: Flow cytometric analysis of apt1, 2 and 3 (ssDNA) affinities to Tg. Affinity analysis of apt1, 2 and 3 to beads coupled with Tg (green, blue and red respectively). A concentration of 500 nM of ssDNA was used. Aptamers were labelled with the Cy5 dye at the 5' end. A non-specific ssDNA (F4 ; yellow) was used as a control (also labelled to Cy5). As a results, only apt1 and apt2 show a higher MFI to beads-Tg than F4 at 500nM. In addition, apt3 and F4 show similar MFI at 500nM.

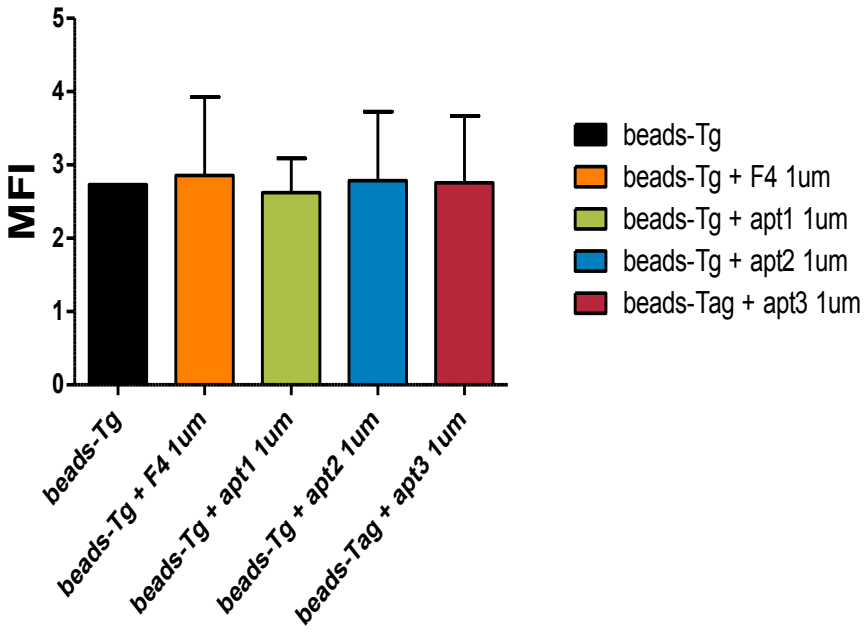

Figure: 10: Flow cytometric analysis of apt1, 2 and 3 (ssDNA) affinities to Tg. Affinity analysis of apt1, 2 and 3 to beads coupled with Tg (green, blue and red respectively). A concentration of 1uM of ssDNA was used. Aptamers were labelled with the Cy5 dye at the 5' end. A non-specific ss DNA (F4 ; yellow) was used as a control (also labelled with Cy5) At 1uM none of the 3 aptamers show a higher MFI as compared to the control. All 3 aptamers plus the control seems to have the same MFI at 1uM.

xxx

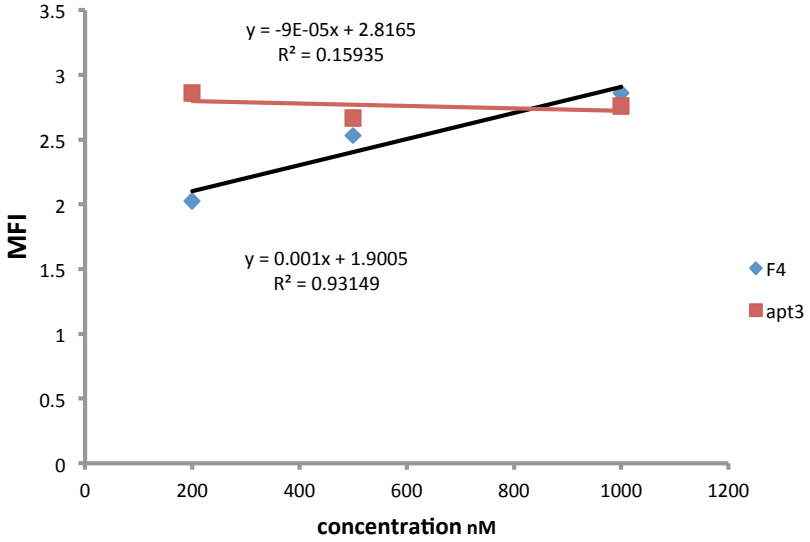

Figure 11: **Scatter plot illustrating the comparative binding of apt3 and the nonspecific ssDNA control (F4) to Tg-Beads at different concentration** (200nM, 500nM and 1 uM). Flow cytometry was use here to measure the MFI. At 200nM apt 3 bound to more beads-Tg than the control. But as we increase its concentration, the affinity of apt3 to Tg-beads slightly change. Also, F4 bind beads-Tg with low affinity as its concentration increase.

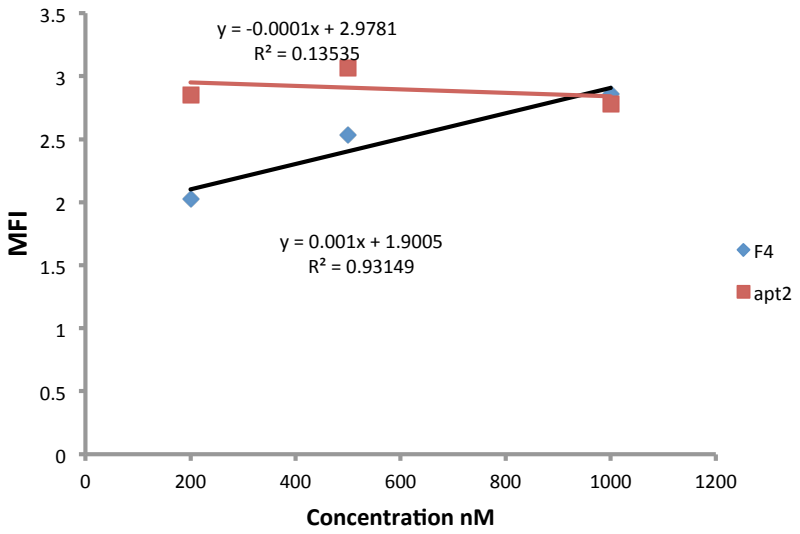

Figure 12: **Scatter plot illustrating the comparative binding of apt2 and the nonspecific ssDNA control (F4) to Tg-Beads at different concentration** (200nM, 500nM and 1 uM). Flow cytometry was use here to mesure the MFI. Here, apt2 show a higher affinity to Tg-beads only at 200nM and 500nM when compare to the control. At 1 uM the control DNA and apt2 showed the same affinity to Tg.

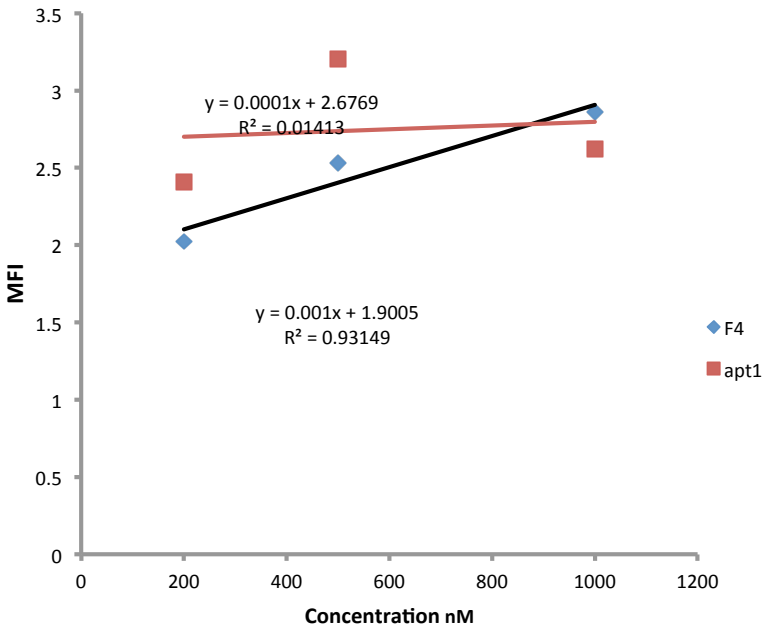

Figure 13: **Scatter plot illustrating the comparative binding of apt 1 and the nonspecific ssDNA control (F4) to Tg-Beads at different concentration** (200nM, 500nM and 1 uM). apt1 and F4 were label with the Cy5 dye at the 5`end and flow cytometry was used to measure the MFI. Here, apt1 show a higher affinity to Tg-beads only at 200nM and 500nM when compare to the control.

Discussion

As we expected, a significantly higher MFI was observed in the presence of Tg coupled with beads (beads-Tg) compared to beads alone when both were incubated with mAb Tg. In fact, we know that monoclonal antibodies are specific to their targets (Spencer et al; 2004). Thus, this confirms the presence of thyroglobulin on the magnetic beads. We also observe in figure 4 that beads alone do not emit any fluorescence as expected. Interestingly, even in the absence of mAb Tg, beads coupled with Tg emit a strong signal (figure 4). This must be due to auto-florescence emitted by Tg because of aromatic amino-acids such as tryptophan and tyrosine in the protein sequence (Yamashita, Y et al; 2003). In addition, the increase in the MFI observed when beads-Tg in the absence of mAb Tg is compared to beads-Tg in the presence of mAb Tg can be explained by the presence of the fluorophore FITC which is coupled to the antibody. Finally, the experiment with beads-MPO was used to see the specificity of mAb Tg to its target. As expected, mAb Tg does not seem to bind MPO.

Comparative affinity analysis of aptamers to beads-Tg and uncoupled beads reveals that apt3 is the best aptamer selected against Tg in contrast to apt1 and apt2.At 200nM apt3 shows the highest affinity for Tg (figures 5, 6 and 7). However, as we increase the concentration of apt3 (up to 1uM), its affinity for Tg was unchanged (figure 7), suggesting that Tg is already saturated by apt3 at 200nM. This trend is usually observed during saturation of a specific biomolecule to its target (Luzi et al; 2003). Interestingly, apt3 binds the uncoupled beads with higher affinity as its concentration is increased although it reaches saturation at 500nM (figure 7). This suggests that apt3 is also able to bind the beads alone although with low affinity at 200nM. Taken together, apt3 binds Tg with a higher affinity than the beads alone.

Although not significant, apt1 seems to bind Tg with a higher affinity at 500nM at which point it reaches saturation (figure 5). Apt2 seems to not show any specific affinity for Tg regardless of its concentration (figure 6). Both apt1 and apt2 seem to bind the beads alone but this was not enhanced by increasing their concentrations (figure 5 and 6). In summary, apt3 recognizes Tg better than apt1 and apt2. When comparing beads and beads-Tg, there was no statistical significance with all 3 aptamers. However, statistical significance was almost reached with apt3 at 200nM ($p=0.0843$, figure 7A). Nevertheless these are promising results and future work involves repeating of this experience (at least 3 times) to generate more samples for statistical analysis to obtain better and more reliable values.

At 200nM, apt3 seems to be more specific to Tg when compare to the negative control F4 (figure 8-10) but this did not reach statistical significance ($p=0.1829$). Also, apt1 and apt2 show their highest affinity for Tg at 500nM (figure 9) when comparing with apt3 and F4. However at 1 uM all aptamers and the control seem to show the same affinity for Tg. In addition, at 200 nM the affinity of apt3 for Tg seems to stabilize as we increase its concentration (figure 11) while the stabilization point for apt1 and apt2 seem to occur after 500nM (figure 12 and 13) suggesting that apt3 has already saturated Tg at 200nM while the saturation of the 2 other aptamers occurs after 500nM. Thus, it takes a lower concentration of apt3 to recognize and saturate Tg when compared to apt1 and apt2 suggesting that apt3 seems to be the more specific and seems to have the lowest K_d of all the 3. However, in order to determine their K_d values, testing at a lower concentration than 200nM should be performed. In addition, triplicates and statistical analysis (student t-test) were made for each experiment. As a result, a similar trend of binding was observed for apt3 upon completion of each individuals experiments (during triplicate) but seems to not be significant ($p = 0.1829$). Nevertheless these are promising results and future work

involves repeating of this experience (more than 3 times) to obtain better and more reliable values. But, it's also possible that not increasing the number of washes and not using a masking buffer to block nonspecific sites on the target can affect the result during the aptamers selection (YanMing Liu et al, 2012).

In addition, F4 seems to binds beads-Tg with lower affinity than beads alone (especially at 200nM) because of the steric hindrance caused by Tg (figures 2 appendix) .Also, as we increase the concentration of F4 its affinity for Tg-beads increase, suggesting that F4 is binding the beads, not Tg which seems to be specific to apt3(figure 10).

As source of errors, the time of incubation of aptamers to Tg were different for one individual experiment during triplicate. Thus, this is a possible explanation for the presence of non-constant values during triplicates (which fail statistical analysis).In the future, a same protocol needs to be used for all experiment in the need to obtain more reliable values.

Future works involve testing the binding analysis at a lower concentration than 200nM to find the actual K_D of all 3 aptamers. Also affinity analysis needs to be performed with multiple repetitions (at least 3 times) in order to obtain significant values. Finally diagnosis with the human serum of DTC patients need to be made, and apt3 seems to be the candidate.

Overall, one of the 3 aptamers (apt3) obtained from a pool selected against TgAb during SELEX was shown to be more specific to Tg when compared to beads and to a nonspecific ssDNA (negative control), thus apt3 is the best candidate for DTC diagnosis in vivo. However additional statistical analyses need to be performed as well as finding their respective K_D in order to confirm this result.

References

1. Nikiforov, Y. E. in Diagnostic Pathology and Molecular Genetics of the Thyroid (eds Nikiforov, Y. E., Biddinger, P. W. & Thompson, L. D. R.) 94–102 (Lippincott Williams & Wilkins, Baltimore, 2009)

2. Chapter 48, "SYNTHESIS OF THYROID HORMONES" in: Walter F., PhD. Boron (2003). *Medical Physiology: A Cellular And Molecular Approach*. Elsevier/Saunders. p. 1300.

3. Zabel, M (December 1984). "Ultrastructural localization of calcitonin, somatostatin and serotonin in parafollicular cells of rat thyroid.". *The Histochemical journal* **16** (12): 1265–72

4. Xing, M. BRAF mutation in thyroid cancer. *Endocr. Relat. Cancer* **12**, 245–262 (2005).

5. Suarez. Presence of mutations in all three ras genes in human thyroid tumors. *Oncogene* **5**, 565–570 (1990)

6. parkin, D. M., Bray, F., Ferlay, J. & Pisani, P. Global cancer statistics, 2002. *CA Cancer J. Clin.* **55**, 74–108 (2005)

7. Chang, Lufen, and Michael Karin. "Mammalian MAP kinase signalling cascades." Nature 410.6824 (2001): 37-40.

8. Yamashita, Alex Shimura, et al. "Notch pathway is activated by MAPK signaling and influences papillary thyroid cancer proliferation." Translational oncology 6.2 (2013): 197.

9. 26. Cully M, You H, Levine AJ, et al. Beyond pten mutations: The pi3k pathway as an integrator of multiple inputs during tumorigenesis. Nat Rev Cancer. 2006;6:184–192.

10. Hou P, Liu D, Shan Y, et al. Genetic alterations and their relationship in the phosphatidylinositol 3-kinase/akt pathway in thyroid cancer. Clin Cancer Res. 2007;13:1161–1170.

11. Davies, Louise, and H. Gilbert Welch. "Increasing incidence of thyroid cancer in the United States, 1973-2002." Jama 295.18 (2006): 2164-2167.

mcadieux 2014-4-10 9:17 AM
Deleted: human

mcadieux 2014-4-10 9:17 AM
Deleted: tumors

mcadieux 2014-4-10 9:16 AM
Formatted: English (CAN)

mcadieux 2014-4-10 9:17 AM
Deleted: tumorigenesis

12. WHO : World Health Organization, International Agency for Research on Cancer, 2012: http://globocan.iarc.fr/

13. PHAC : Canadian Cancer Society, Canadian Cancer Statistics, 2011: http://www.phac-aspc.gc.ca/cd-mc/cancer/cancer_thyroid-thyroide-eng.php

14. Santarpia, Libero, et al. "Phosphatidylinositol 3-kinase/akt and ras/raf-mitogen-activated protein kinase pathway mutations in anaplastic thyroid cancer." Journal of Clinical Endocrinology & Metabolism 93.1 (2008): 278-284**.**

15. Tubiana M, Schlumberger M, Rougier P, Laplanche A, Benhamou E, Gardet P, Caillou B, Travagli JP, Parmentier C (1985) Long-term results and prognostic factors in patients with differentiated thyroid carcinoma. *Cancer* **55**: 794–804.

16. Schlumberger, M., Berg, G., Cohen, O., Duntas, L., Jamar, F., Jarzab, B., ... & Wiersinga, W. M. (2004). Follow-up of low-risk patients with differentiated thyroid carcinoma: a European perspective. European Journal of Endocrinology, 150(2), 105-112.

17. Spencer, C. A., Takeuchi, M., Kazarosyan, M., Wang, C. C., Guttler, R. B., Singer, P. A., ... & Nicoloff, J. T. (1998). Serumum Thyroglobulin Autoantibodies: Prevalence, Influence on Serumum Thyroglobulin Measurement, and Prognostic Significance in Patients with Differentiated Thyroid Carcinoma 1. Journal of Clinical Endocrinology & Metabolism, 83(4), 1121-1127.

18. Malthiéry, Y., Marriq, C., Bergé-Lefranc, J. L., Franc, J. L., Henry, M., Lejeune, P. J., ... & Lissitzky, S. (1989). Thyroglobulin structure and function: recent advances. *Biochimie*, *71*(2), 195-209.

19. Venturi S, Donati FM, Venturi A, Venturi M (August 2000). "Environmental iodine deficiency: A challenge to the evolution of terrestrial life?". *Thyroid* **10** (8): 727–9.

20. Boron WF (2003). Medical Physiology: A Cellular And Molecular Approaoch. Elsevier/Saunders. p. 1300. ISBN 1-4160-2328-3

21. Deshpande, V., & Venkatesh, S. G. (1999). Thyroglobulin, the prothyroid hormone: chemistry, synthesis and degradation. Biochimica et Biophysica Acta (BBA)-Protein Structure and Molecular Enzymology, 1430(2), 157-178.

22. Cooper, D. S., Doherty, G. M., Haugen, B. R., Kloos, R. T., Lee, S. L., Mandel, S. J. & Tuttle, R. M. (2009). Revised american thyroid association management guidelines for patients with thyroid

mcadieux 2014-4-10 9:16 AM
Deleted: um

mcadieux 2014-4-10 9:16 AM
Deleted: um

mcadieux 2014-4-10 9:24 AM
Deleted: Serum

mcadieux 2014-4-10 9:24 AM
Deleted: Serum

mcadieux 2014-4-10 9:11 AM
Deleted: nm

nodules and differentiated thyroid cancer: the american thyroid association (ATA) guidelines taskforce on thyroid nodules and differentiated thyroid cancer. Thyroid, 19(11), 1167-1214.

23. Torrens JI, Burch HB: Serum Thyroglobulin measurement. Utility in Clinical Practice. Endocrinol Metab Clin North AM 2001 June;30(2):429-467

24. Spencer, C. A. (2004). Challenges of serum thyroglobulin (Tg) measurement in the presence of Tg autoantibodies. *Journal of Clinical Endocrinology & Metabolism*, *89*(8), 3702-3704.

25. Jayasena, S. D. (1999). Aptamers: an emerging class of molecules that rival antibodies in diagnostics. Clinical chemistry, 45(9), 1628-1650.

26. Vitreschak, A. G., Rodionov, D. A., Mironov, A. A., & Gelfand, M. S. (2004). Riboswitches: the oldest mechanism for the regulation of gene expression?. TRENDS in Genetics, 20(1), 44-50.

27. Brody, E. N., & Gold, L. (2000). Aptamers as therapeutic and diagnostic agents. Reviews in Molecular Biotechnology, 74(1), 5-13.

28. Daniels, D. A., Chen, H., Hicke, B. J., Swiderek, K. M., & Gold, L. (2003). A tenascin-C aptamer identified by tumor cell SELEX: systematic evolution of ligands by exponential enrichment. Proceedings of the National Academy of Sciences, 100(26), 15416-15421.

29. Huang, Z., & Szostak, J. W. (2003). Evolution of aptamers with a new specificity and new secondary structures from an ATP aptamer. Rna, 9(12), 1456-1463.

30. Osborne, S. E., Matsumura, I., & Ellington, A. D. (1997). Aptamers as therapeutic and diagnostic reagents: problems and prospects. Current opinion in chemical biology, 1(1), 5-9.

31. Walsh, R.; M. DeRosa (2009). "Retention of function in the DNA homolog of the RNA dopamine aptamer.". Biochemical and Biophysical Research Communications 388: 732–735.

32. Min, K.; M. Cho, S. Han, Y. Shim, J. Ku, C. Ban (2008). "A simple and direct electrochemical detection of interferon-gamma using its RNA and DNA aptamers.". *Biosensors & Bioelectronics* **23**: 1819–1824

33. Potty, A.; K. Kourentzi, H. Fang, G. Jackson, X. Zhang, G. Legge, R. Willson (2009). "Biophysical Characterization of DNA Aptamer Interactions with Vascular Endothelial Growth Factor.". Biopolymers91: 145–156

mcadieux 2014-4-10 9:24 AM
Deleted: Serum

mcadieux 2014-4-10 9:24 AM
Deleted: serum

mcadieux 2014-4-10 9:16 AM
Deleted: um

mcadieux 2014-4-10 9:16 AM
Formatted: French (Canada)

mcadieux 2014-4-10 9:16 AM
Deleted: um

mcadieux 2014-4-10 9:16 AM
Formatted: French (Canada)

34. Savory, N., Abe, K., Sode, K., & Ikebukuro, K. (2010). Selection of DNA aptamer against prostate specific antigen using a genetic algorithm and application to sensing. *Biosensors and Bioelectronics*, *26*(4), 1386-1391.

35. Proske, D., Blank, M., Buhmann, R., & Resch, A. (2005). Aptamers—basic research, drug development, and clinical applications. Applied microbiology and biotechnology, 69(4), 367-374.

36. Sundaram, P., Kurniawan, H., Byrne, M. E., & Wower, J. (2013). Therapeutic RNA aptamers in clinical trials. European Journal of Pharmaceutical Sciences, 48(1), 259-271.

37. Luzi, E., Minunni, M., Tombelli, S., & Mascini, M. (2003). New trends in affinity sensing: aptamers for ligand binding. TrAC Trends in Analytical Chemistry, 22(11), 810-818.

38. Liu, Y., Wang, C., Li, F., Shen, S., Tyrrell, D. L. J., Le, X. C., & Li, X. F. (2012). DNase-mediated single-cycle selection of aptamers for proteins blotted on a membrane. Analytical chemistry, 84(18), 7603-7606.

39. Yamashita, Y., & Tanoue, E. (2003). Chemical characterization of protein-like fluorophores in DOM in relation to aromatic amino acids. Marine Chemistry, 82(3), 255-271.

Appendix

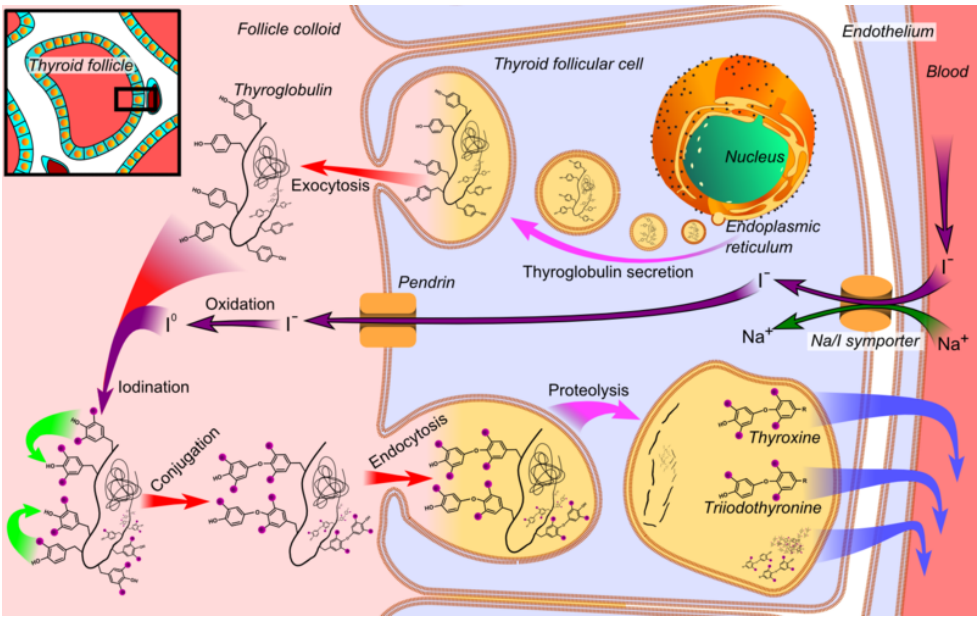

Fig 1 (Boron WF; 2003) :Synthesis of the thyroid hormones. As seen on an individual thyroid follicular cell: Thyroglobulin is synthesized in the rough endoplasmic reticulum and follows the secretory pathway to enter the colloid in the lumen of the thyroid follicle by exocytosis. Meanwhile, a sodium-iodide (Na/I) symporter puMps iodide (I-) actively into the cell, which previously has crossed the endotheliuM by largely unknown mechanisms.This iodide enters the follicular lumen from the cytoplasm by the transporterpendrin, in a purportedly passive manner. In the colloid, iodide (I-) is oxidized to iodine (I0) by an enzyme called thyroid peroxidase.Iodine (I0) is very reactive and iodinates the thyroglobulin at tyrosyl residues in its protein chain (in total containing approximately 120 tyrosyl residues).In conjugation, adjacent tyrosyl residues are paired together.Thyroglobulin binds the megalin receptor for endocytosis back into the follicular cell.Proteolysis by various proteases liberates thyroxine and triiodothyroninemolecules, which enter the blood by largely unknown mechanisms.

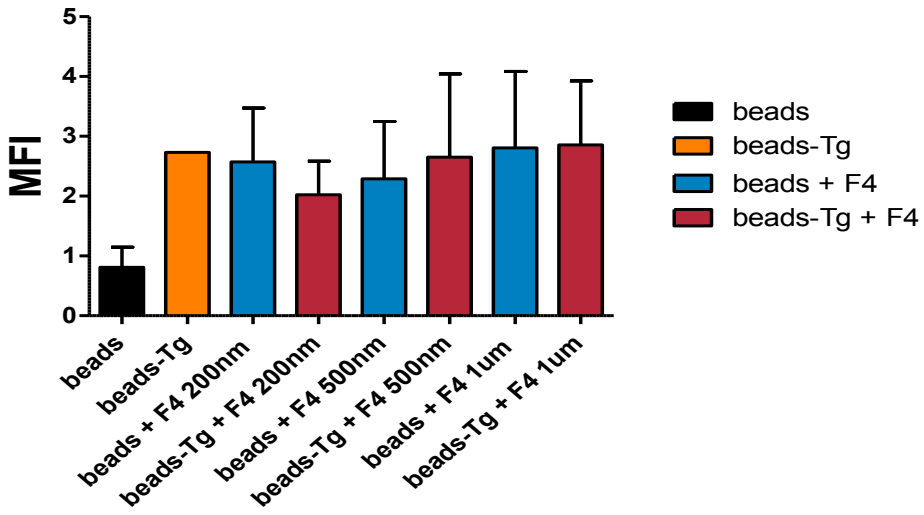

Figure2: Flow cytometric analysis of a nonspecific ssDNA control to TgAb. Comparative binding of F4 (to beads coupled with Tg (red) and beads alone (blue) at different concentration. F4 was labelled with the Cy5 dye at the 5' end and affinity analysis was made by flow cytometry.